



Natural Resources  
Canada      Ressources naturelles  
Canada

**GEOLOGICAL SURVEY OF CANADA  
OPEN FILE 8913**

**Chemostratigraphic logging of the Lower  
Ordovician and Precambrian, Bells  
Corners Borehole Calibration Facility,  
Ottawa, Ontario**

**L.C. Olson, R.D. Knight, H.L. Crow, and H.A.J. Russell**

**2022**

**Canada**



ISSN 2816-7155  
ISBN 978-0-660-44934-0  
Catalogue No. M183-2/8913E-PDF

## GEOLOGICAL SURVEY OF CANADA OPEN FILE 8913

# Chemostratigraphic logging of the Lower Ordovician and Precambrian, Bells Corners Borehole Calibration Facility, Ottawa, Ontario

**L.C. Olson<sup>1</sup>, R.D. Knight<sup>2</sup>, H.L. Crow<sup>2</sup>, and H.A.J. Russell<sup>2</sup>**

<sup>1</sup>35 Cleadon Drive, Ottawa, Ontario

<sup>2</sup>Geological Survey of Canada, 601 Booth Street, Ottawa, Ontario

**2022**

© Her Majesty the Queen in Right of Canada, as represented by the Minister of Natural Resources, 2022

Information contained in this publication or product may be reproduced, in part or in whole, and by any means, for personal or public non-commercial purposes, without charge or further permission, unless otherwise specified.

You are asked to:

- exercise due diligence in ensuring the accuracy of the materials reproduced;
- indicate the complete title of the materials reproduced, and the name of the author organization; and
- indicate that the reproduction is a copy of an official work that is published by Natural Resources Canada (NRCan) and that the reproduction has not been produced in affiliation with, or with the endorsement of, NRCan.

Commercial reproduction and distribution is prohibited except with written permission from NRCan. For more information, contact NRCan at [copyright-droitdauteur@nrcan-rncan.gc.ca](mailto:copyright-droitdauteur@nrcan-rncan.gc.ca).

Permanent link: <https://doi.org/10.4095/330519>

This publication is available for free download through GEOSCAN (<https://geoscan.nrcan.gc.ca/>).

### Recommended citation

Olson, L.C., Knight, R.D., Crow, H.L., and Russell, H.A.J., 2022. Chemostratigraphic logging of the Lower Ordovician and Precambrian, Bells Corners Borehole Calibration Facility, Ottawa, Ontario; Geological Survey of Canada, Open File 8913, 1 .zip file. <https://doi.org/10.4095/330519>

Publications in this series have not been edited; they are released as submitted by the author.

## Table of Contents

1.0 Introduction .....	1
Background .....	1
Objectives and Scope .....	2
2.0 Geological Setting .....	4
Precambrian Bedrock (core depth 120.12 - 64.30m) .....	4
Keeseville Formation (core depth 64.30 - 20.45m) .....	4
Theresa and Beauharnois Formations (core depth 20.45 – 5.30m).....	5
3.0 Sample Collection and Analytical Methods.....	7
pXRF analyses.....	8
Paired pXRF and laboratory chemical analyses.....	9
Data Delivery .....	11
Data Processing.....	11
4.0 Geochemical Results .....	14
Precambrian Bedrock (core depth 120.12 - 64.30m) .....	14
Keeseville Formation (core depth 64.30 - 20.45m) .....	15
Theresa and Beauharnois Formations (core depth 5.30 – 20.45m).....	16
5.0 Summary and conclusions.....	19
6.0 Acknowledgements .....	19
7.0 References .....	19

## **Abstract**

Geochemical data were collected from a 120-meter-deep borehole (BC81-2) located at the Geological Survey of Canada's Bells Corners Borehole Calibration Facility in Ottawa, Ontario. This report documents geochemical data collected for the most frequently logged of the six boreholes located at the facility. The geochemical data were collected using a portable X-ray fluorescence (pXRF) spectrometer with a subset of samples collected for modern laboratory based fusion and multi-acid methods to calibrate the pXRF data for improved accuracy. Borehole geochemistry provides a characterization of Precambrian and overlying Ordovician rocks in the Ottawa area that augments the understanding of geophysical properties obtained from the calibration borehole. The combined geochemical and geophysical datasets further define rock characteristics, formation boundaries, as well as alteration zones. The results demonstrate the usefulness of pXRF derived geochemical data and chemostratigraphy of rock cores. The chemostratigraphic data augment data collected with spectral gamma logging tools and support an enhanced interpretation of geological contacts across transitional boundaries and the nature of the matrix mineralogy.

## **1.0 Introduction**

Chemostratigraphy entails the characterization of rock stratigraphy using chemical classification of rock (Craigie, 2018). Chemostratigraphy was not part of standard research carried out by geologists or geophysicists until the mainstream scientific acceptance of the modern, cost-effective, non-destructive, pXRF spectrometry tool. Portable X-ray fluorescence spectrometry (pXRF) has revolutionized the gathering of geochemical data and opened new avenues of research and applications in mineral exploration (oil and gas and mineral), environmental surveys, and validation of other analytical tools such as downhole geophysics. Ongoing advances in pXRF technology have resulted in the ability to collect geochemical data that would otherwise be beyond the financial scope of many projects where traditional laboratory geochemical analysis (i.e., comprehensive aqua regia, plus multi acid, plus fusion digestions followed by inductively coupled plasma-mass spectrometry (ICP-MS/ES)), can cost ~100\$/sample. Besides being cost effective, the spectrometer is an excellent tool for real-time analyses for a suite of elements ranging from magnesium (Mg) to uranium (U). The development of pXRF as a mainstream geochemical analytical tool is summarized in Glanzman and Closs (2007), updated by Lemiere (2018), and compared with results from traditional laboratory methods by Rouillon and Taylor (2016). An overview of best practices for the collection of geochemical data using pXRF is presented in Knight et al. (2021).

## **Background**

The Bells Corners borehole calibration facility was established in the late 1970's by the Geological Survey of Canada (GSC) for the development and calibration of geophysical instruments and to evaluate new technologies. The site is located on the campus of the Canada Centre for Mineral and Energy Technology (CANMET) research laboratories in Bells Corners, a suburb of Ottawa, Ontario, (Figure 1 and 2). Revitalization of the borehole facility was initiated in 2019, allowing for a new suite of physical, mechanical, and hydrological calibration data to be collected, including water level and precipitation monitoring (Crow et al., 2021). This is expanding the site's potential beyond the historic mineral exploration downhole geophysical applications. Deployment of new geophysical tools was undertaken with a view to understanding the connection between the physical properties of the rock and the hydrogeology of fracture and matrix groundwater flow (e.g., Pehme et al., 2022). These new datasets contain high-resolution imagery with optical and acoustic televiewers, providing context for studying

hydrogeological conditions at the site, alongside repeat groundwater temperature, conductivity and flow logs, and nuclear magnetic resonance measurements (Crow et al., 2021).

Detailed information about the Bells Corners Borehole Calibration Facility is provided in, Killeen and Conway (1978), Killeen et al., 1984; Killeen, 1986, Mwenifumbo et al. (2005), and Crow et al. (2021).

## Objectives and Scope

Geochemical characterization of Precambrian and Ordovician rock core was undertaken to supplement the well documented downhole geophysical characteristics of the Bells Corners Calibration Facility. The primary objective of this open file is to release geochemical data for borehole BC81-2 (Fig. 3). Further to the primary objective, this study examines:

- assessment of pXRF for the characterization of bedrock core stored in core trays,
- the potential for chemostratigraphy to define rock type and formation boundaries,
- the accuracy of pXRF data acquired from granitic and carbonate basin rocks compared to traditional laboratory methods.

To characterize the chemostratigraphy, a relatively high-resolution set of geochemical data was acquired using a portable X-ray fluorescence spectrometer (pXRF) using similar methods of Lawley et al. (2015). The data presented here augments downhole geophysical data, lithology, grain-size, and groundwater properties (Crow et al., 2021) and provides a platform to further define the Precambrian basement and the overlying Cambrian and Ordovician sedimentary sequence

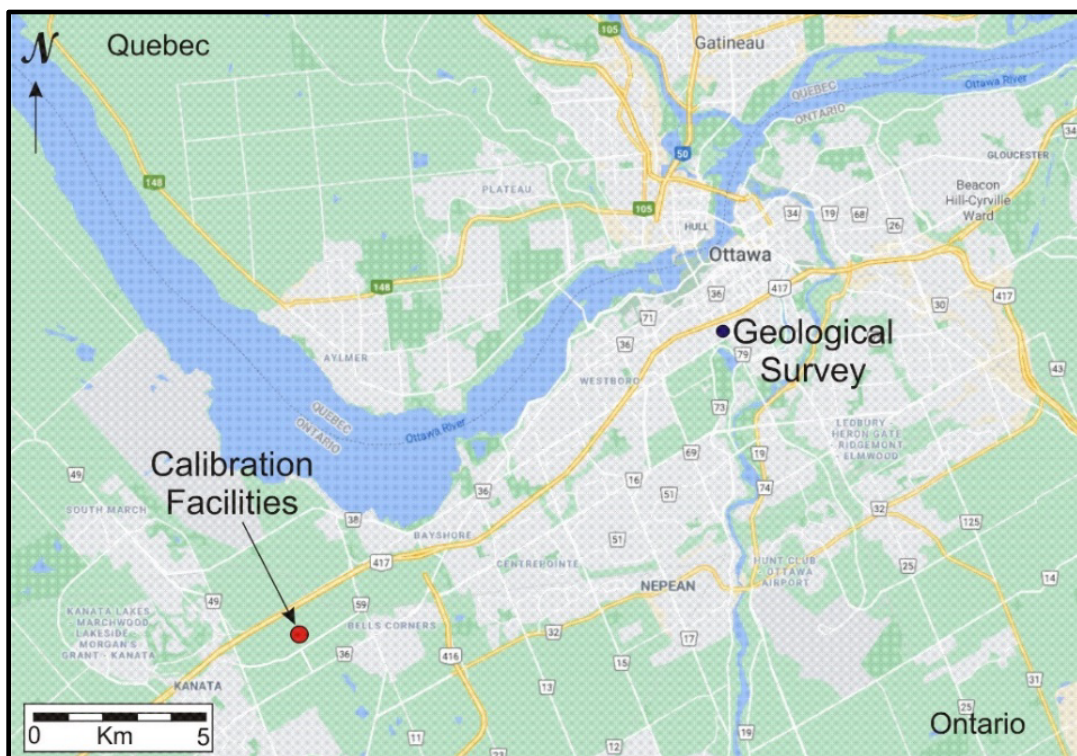


Figure 1. Location of the Bells Corners Borehole Calibration Facility and the main offices of the Geological Survey of Canada, Booth Street Complex in Ottawa.

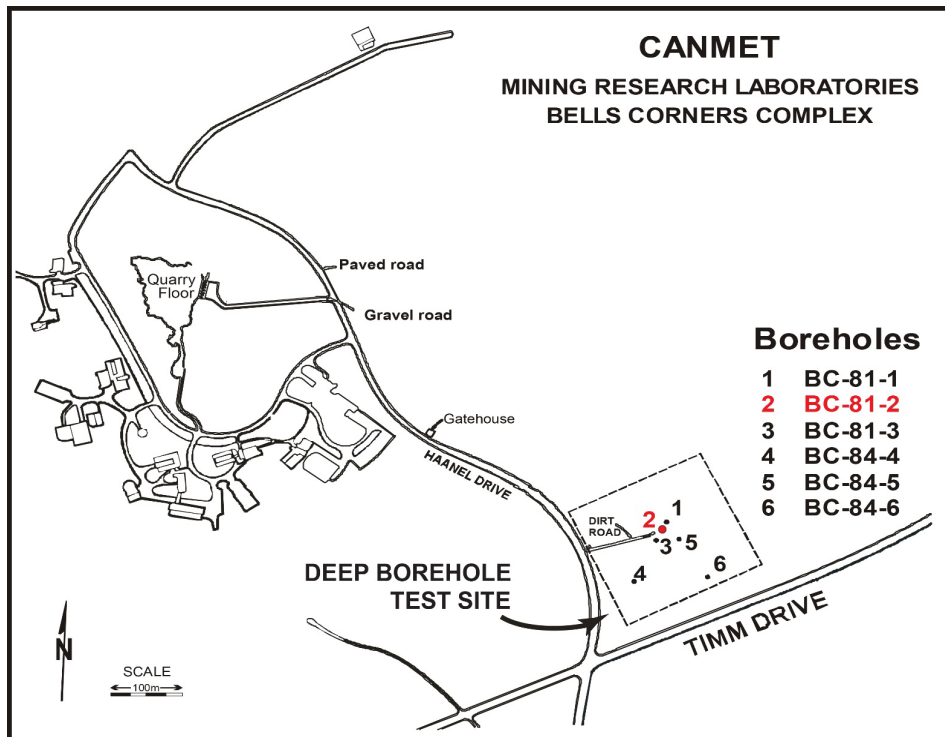


Figure 2: Location of the borehole calibration facility within the Bells Corners CANMET mining research laboratories complex.

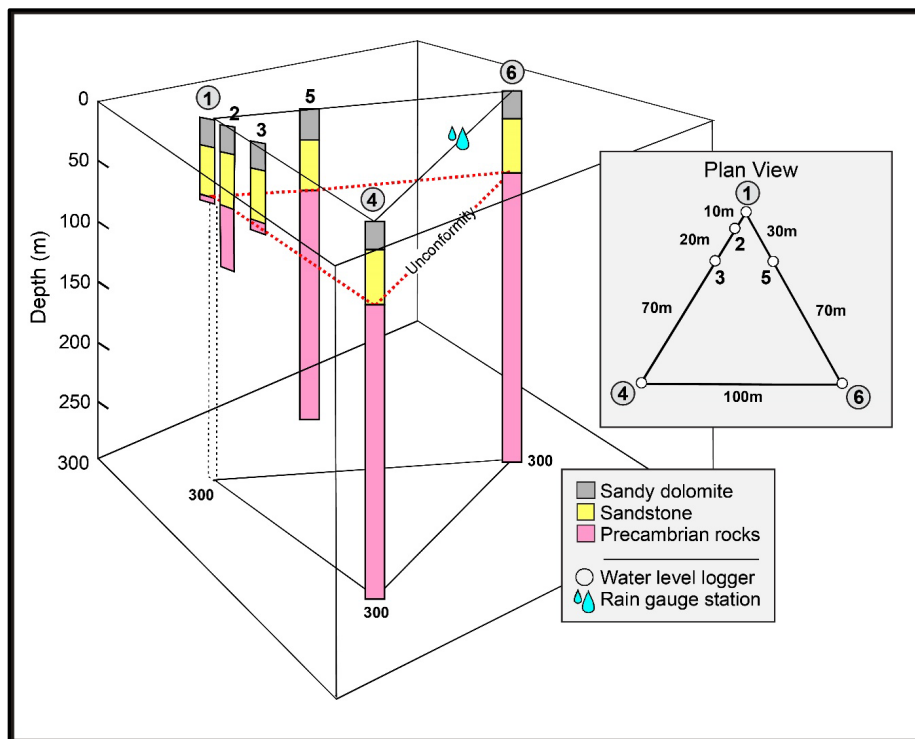


Figure 3: Configuration of boreholes and depths at the Bells Corners Calibration Facility (from Crow et al., 2021).

## 2.0 Geological Setting

The boreholes intersect Mesoproterozoic rocks (0.9 – 1.6 Ga; Hofmann, 1998; Davidson, 1998), of the Central Metasedimentary Belt (Wynne-Edwards, 1972; Easton, 1992; Davidson, 1998), and Paleozoic sedimentary rocks assigned to the Potsdam and Beekmantown Groups, (Fig. 4; Bernius, 1996). Resistivity, density, and gamma logs are shown alongside the borehole stratigraphy in Figure 5 and Appendix C. These logs show the differentiation of Precambrian rocks, Ordovician formation transitions and boundaries. The Mesoproterozoic to Lower Ordovician contact comprises a well-defined regional unconformity that spans a period of 0.5Ga (Di Prisco and Springer, 1991), shown in Figures 4 and 5.

Mesoproterozoic rocks consist mainly of undeformed potassic syenites and granites, dated to 1.1Ga (Corriveau et al., 1990), pegmatite, mafic chlorite-gneiss, and biotite-hornblende-scapolite gneiss – all of which have complex structural relationships that cannot be traced between the boreholes at the site (Bernius, 1996).

The overlying the Potsdam and Beekmantown Group rocks consist of carbonate, and sandstone, with a wide variety of structures and physical and mineralogical properties. The Potsdam Group, which outcrops extensively in Ontario, Quebec and Upper New York state, consists of sandstones and conglomerates first reported by Emmons (1838) and studied extensively since (e.g., see Salad Hersi et al., 2002; Dix et al., 2004; Landing et al., 2009; Sanford, 2007; Sanford and Arnott, 2010; Lowe, 2016 and references therein). U-Pb dating indicate the sediments were derived from the rocks of the Central Metasedimentary Belt and more distant terranes of the Grenville Province (Chiarenzelli et al., 2010; Sanford and Arnott, 2010; Lowe et al., 2018).

### Precambrian Bedrock (core depth 120.12 - 64.30m)

The 120-m deep borehole (BC81-2, Fig. 3) intersects a suite of Precambrian igneous and metasedimentary rocks that can vary significantly over relatively short decimeter-scale intervals (Bernius, 1996). From the base of the borehole to approximately 90m depth, rocks consist of predominantly mafic chlorite gneiss and biotite-hornblende-scapolite gneiss with three significant intervals of fresh syenite and one thin interval of pegmatite (Figure 4F). From a depth of 90m to the contact with the overlying Paleozoic sediments, the rock is characterized by more felsic granite and gneiss (Figure 4E). The uppermost 17m of granite and gneiss comprises an alteration zone consisting of sericite, clay minerals, chlorite, epidote, hematite and calcite along with quartz and plagioclase (Bernius, 1996).

Above this alteration zone, from 64.8 - 64.3m, rock consists of irregular, broken, highly weathered syenite and granite with friable pinkish-red clay and altered feldspars, and greenish grey saprolite derived from mafic gneiss. Bernius (1996) has classified this alteration zone as a saprolite or regolith. The contact of the Precambrian rocks with the overlying sedimentary sequence represents a sharp regional unconformity.

### Keeseeville Formation (core depth 64.30 - 20.45m)

The Keeseeville Formation (locally known as the Nepean Formation) is comprised of fine- to coarse-grained sandstone with cross bedding or bioturbation, and massive white sandstone (quartz arenite). The contact with the underlying Precambrian rocks consists of 18cm of quartz conglomerate with minor brown limonitic horizons (Bernius, 1996). Overlying the conglomerate is a 5.2-m interval of white quartz sandstone which in turn is overlain by alternating bioturbated and cross-bedded sandstone, with variable amounts of hematite (iron staining), glauconite and limonite (Figure 4D, ~56 to 37m). There are 23 bioturbated layers identified, ranging in thickness from 5 – 83 cm. The alternating bioturbated and

crossbedded sandstone is overlain by a 57cm thick shaly sandstone horizon. The upper 16m of the Keeseville Formation consists of a massive, white quartz arenite with minor dark laminae and irregular layers (Figure 4C). The contact between the Keeseville Fm. and the overlying Theresa Formation (known locally as the March Formation) is documented as transitional by Sanford and Arnott (2010), or as a disconformity caused by a regional hiatus in sedimentation by Dix et al. (2004).

### **Theresa and Beauharnois Formations (core depth 20.45 – 5.30m)**

The Theresa Formation represents the lowermost unit of the Beekmantown Group and consists primarily of dolomitic sandstone, sandy coarse-grained quartz arenite with horizons of fine-grained quartzose dolostone (Bernstein, 1992; Salad Hersi et al., 2003). The Theresa Formation represents a transitional lithology, from the underlying quartz-rich Keeseville Formation to the overlying dolomitic Beauharnois Formation (Bernstein, 1992; Salad Hersi et al., 2003). The local thickness of the Theresa Formation has been interpreted to be about 10m. In borehole BC81-2, the base of the Theresa Formation contains distinct dark grey layer of thucolite, a U-Th bearing and chalcopyrite-rich pyrobitumen (Figure 4B) (Hoekstra and Fuchs, 1960; Charbonneau et al., 1975; Bernius, 1996). Overlying the thucolite is a dolomitic sandstone with minor crossbedding. The dolomitic sandstone is in turn overlain by a variable textured, reddish to greenish grey, sandy dolostone.

At a depth of approximately 11m the core begins to transition upward into grey, fine to medium crystalline dolostone, with minor very thin interbeds of fine-grained quartz sandstone (Figure 4A). Cavities in the uppermost sandy dolomite are filled with calcite. Rock comprising the upper several metres of core are broken and fractured with visible weathering along vertical fracture surfaces.

The Theresa Formation is overlain by sediments that represent a transition to the Beauharnois Formation (locally known as the Oxford Formation). Although extensively studied (see Bernstein, 1992 and references therein) key boundaries and chemostratigraphic transitions between the Keeseville, Theresa and Beauharnois Formations remain unresolved. The Beauharnois Formation represents the uppermost sediments observed in borehole BC81-2 and consists of dolostone with subordinate amounts of limestone, quartzose carbonate, and dolomitic and calcareous arenite (Bernstein, 1992).

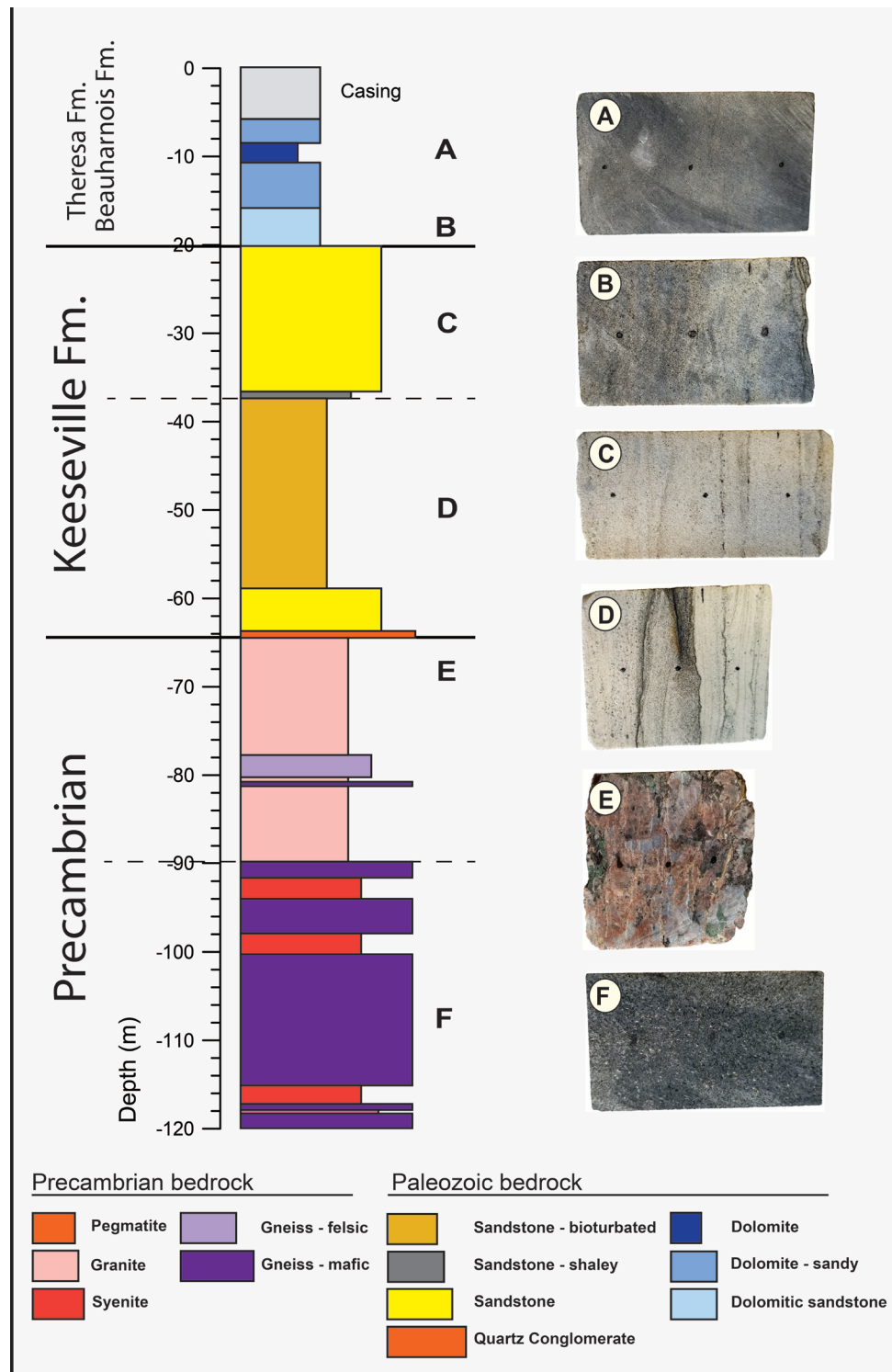


Figure 4: Illustration of BC81-2 lithologies with representative photographs. The black dots on the photographs represent pXRF analysis locations and are separated by 2.5 – 3.0 cm. Sample photographs are orientated 90 degrees to vertical with top to the left. Wireline depths used. Rock lithologies modified from Crow et al., 2021. Photographs by L.C. Olson. NRCan photograph DB numbers: 4A- 2022-300; 4B-2022-301; 4C-2022-302 ; 4D-2022-303 ; 4E-2022-304 ; 4F-2022-305 .

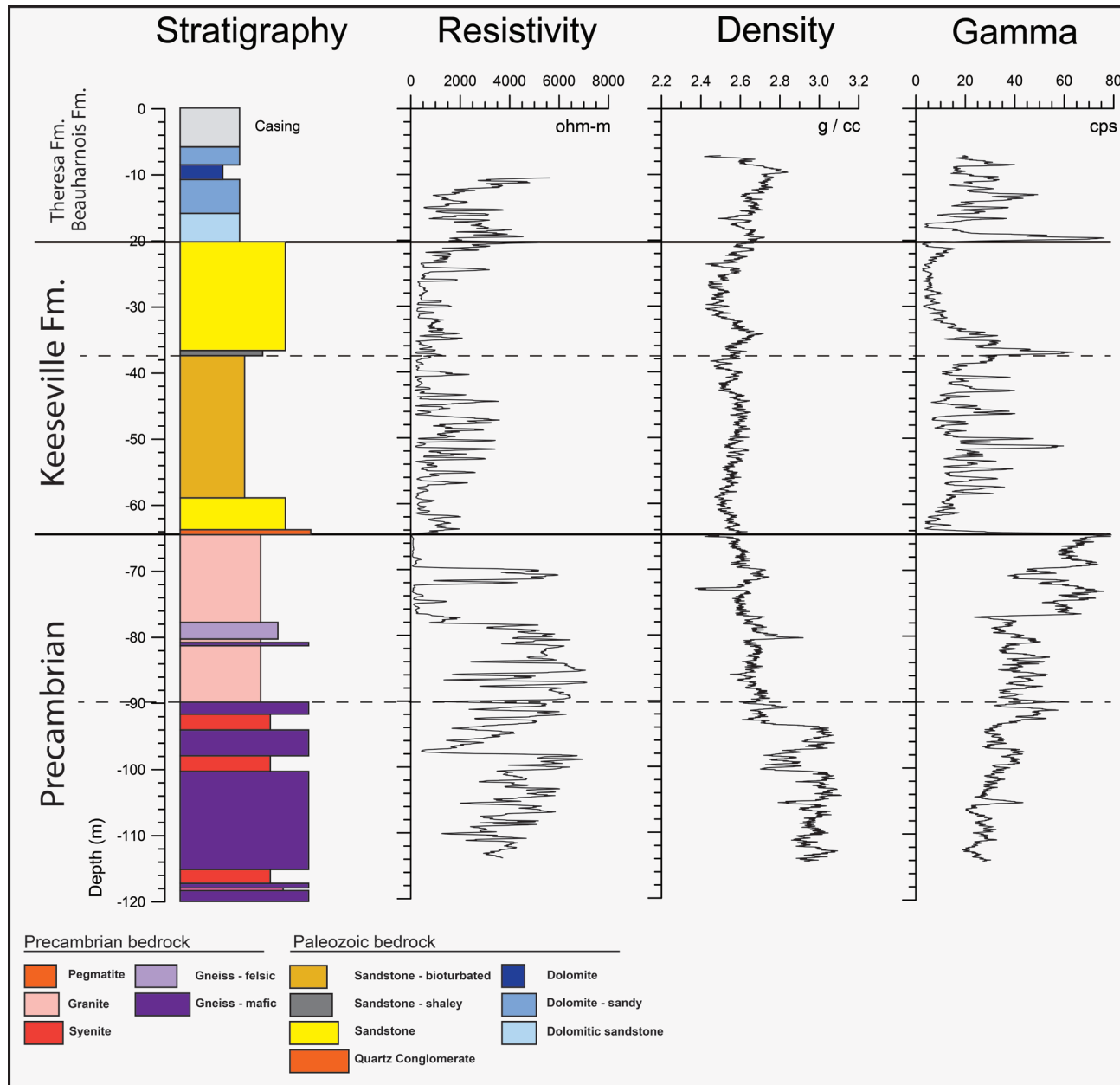


Figure 5: Illustration of BC81-2 lithologies with downhole geophysical logs for resistivity, density, and gamma. Wireline depths used. Rock lithologies modified from Crow et al., 2021.

### 3.0 Sample Collection and Analytical Methods

The BC81-2 drill core is stored in 19 core boxes and has a total length of approximately 115 meters.. At time of drilling, depth marks were scribed along the core at 10cm intervals. During geophysical logging of borehole BC81-2, differences between core depths and calibrated wireline depths were noted. To accommodate these differences, a depth correction has been developed to relate core depths to calibrated geophysical log depths (see Crow et al., 2021 for details). Spreadsheets of pXRF data (Appendix A)

contain both core and wireline depths (in metres below ground surface) to allow for comparison of pXRF data with geophysical logs.

One of the secondary objectives of this research is to evaluate if rock core can be analyzed without removal from the core tray. To meet this objective, the pXRF spectrometer was mounted in a custom-modified drill press with an adjacent tabletop roller system (Figure 6). The roller system allows the core box to be moved horizontally under the spectrometer. The modified drill-press allows for the spectrometer to be raised to advance the core to the next analytical site and then lowered to be in contact with the rock surface. Prior to analyses the core was washed with distilled water to remove dust and other possible contaminants from the core surface. A camera in the spectrometer displays the analytical site on the built-in monitor to ensure that a representative area of rock is being examined and not just a large individual mineral. During visual examination of the image, consideration must be taken for the possibility of edge effects as described by Knight et al. (2002) and recorded in the analytical sample site notes.

### **pXRF analyses**

Geochemical analyses by pXRF were collected between December 5 to 19, 2019, and January 7 to 10, 2020. Analytical data were obtained from the rock core starting at a depth of 5.80m, with subsequent analyses every 30cm to the base of the borehole, and every 10 – 20cm, for areas of special interest. The final analysis was taken at a core depth of 120.10m for a total of 404 records resulting in a high-resolution geochemical dataset for the borehole.

Data were acquired using a handheld Thermo Scientific Niton XL3t GOLDD spectrometer equipped with a Cygnet 50 kV, 2-watt, Ag Anode X-ray tube and a XL3 silicon drift detector (SDD) with 180 000 counts per second (cps) throughput. Data were collected in Mining Mode Cu/Zn using 4 filters: High and Main (50kv/40  $\mu$ A max), differentiated by filter material composition and thickness; Low (20kv/100  $\mu$ A max); and Light (8kv/200  $\mu$ A max). All standard reference materials and core intervals were analyzed with a dwell time of 45 seconds per filter for a total of 180s per analysis utilizing an un-collimated 8mm window with NITON pre-set factory specifications calibrated to convert counts to concentrations.

Prior to pXRF data collection the spectrometer housing was cleaned with compressed air, distilled water and Kimwipes®. A daily internal system check of the spectrometer was completed to ensure proper functioning of the instrument. Although considerable research has been carried out at the GSC using a pXRF for quantifying the geochemistry of Quaternary sediments (Knight et al., 2021) only limited research has been carried out on rock cores (Lawley et al., 2015). Consequently, a suit five references materials with well documented pXRF geochemistry from previous Quaternary research (Knight et al., 2021) were analyzed at the start and end of each data collection session to ensure that the spectrometer was operating at optimal performance, a Teflon blank, a SiO<sub>2</sub> blank (Si DP 6000), two CANMET certified reference materials, Till-1 and Till-2, and a GSC internal till standard reference sample TCA 8010 were analyzed. All reference materials, except for the Teflon Blank, were covered with 4 $\mu$ m thick Chemplex® Prolene® film. Every 20 samples the Till-1, Till-4 and TCA 8010 were re-tested.

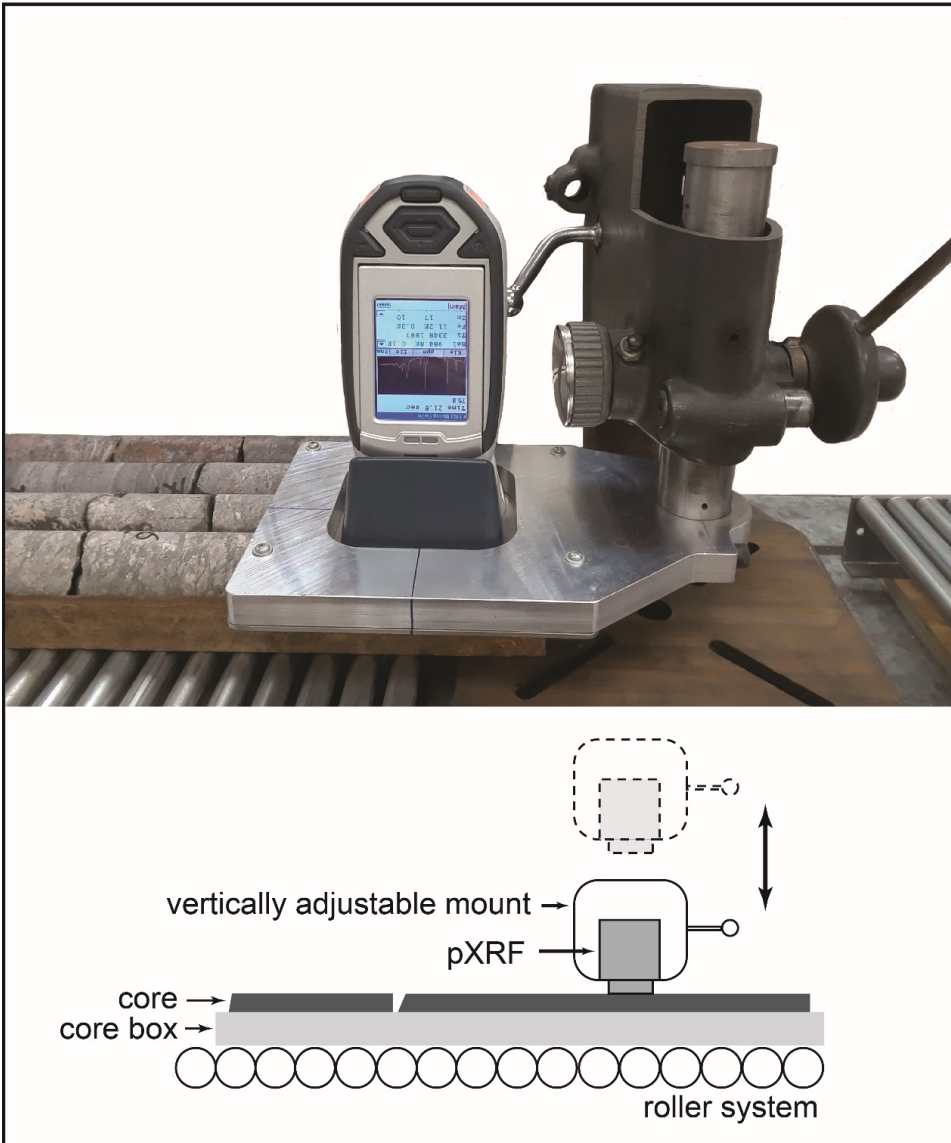


Figure 6: Illustration of pXRF spectrometer mounted in a custom test stand with the ability to raise and lower the spectrometer to be in contact with the sample surface. Core boxes are moved under the spectrometer using a roller system. Photograph by H.L. Crow. NRCan photograph DB numbers: 2022-306.

### **Paired pXRF and laboratory chemical analyses**

To provide insight into the accuracy of the pXRF data acquired from granitic and carbonate basin rocks, 30 representative core samples were selected for traditional laboratory ICP-MS/ES analysis, 12 from the Precambrian basement, 8 from the Keeseeville Formation, and 10 from the Theresa and Beauharnois Formations. The comparison of pXRF chemistry to traditional laboratory methods provides the basis for increasing the accuracy of pXRF elemental data that fall outside the criteria for definitive and quantitative data as discussed in Knight et al. (2021). Samples were cut from the core, ranging in length from 3.60cm to 9.70cm with an average length of 6.72cm, and split in half length wise. One half of the sample was sent

to Bureau Veritas Commodities Canada Ltd in Vancouver, BC for processing and analyses in February 2020, the other half was returned to the core box for pXRF analyses.

On the other half of the cut samples, pXRF analyses were carried out on the cut surface unless the surface was rough. The rough-cut surface of the sample does not allow complete contact of the spectrometer with the sample. In order to account for variations in mineralogy, grain size and other heterogeneous features, three closely spaced pXRF analyses were collected from each of the 30 representative samples. Reading locations are shown by the black dot markings in Figure 7. The mean of the three pXRF concentrations was calculated and subsequently compared to traditional laboratory data to calibrate the pXRF data set. The pXRF spectrometer data were obtained from each sample in order to use the results to develop calibration equations with the lab chemistry to improve the accuracy of the pXRF analyses. Photographs of the intact core, cut and uncut surface and analytical sites for pXRF-spectrometry are presented in Appendix D, Core\_Sample\_photographs.pdf

For laboratory analyses, two laboratory analytical methods were employed: 1) a 4-acid, hot dissolution in HNO<sub>3</sub>-HClO<sub>4</sub>-HF taken to dryness and then the residue dissolved in HCl, followed by ICP-MS analysis; 2) combining the sample with lithium metaborate/tetraborate to create a fusion disc followed by digestion in dilute nitric acid, and analysis by ICP-ES (major elements) and ICP-MS (trace elements). Laboratory analysis using aqua-regia (partial digestion)- a popular geochemical method used in mineral exploration - where not obtained as they are not valid for comparative purposes with analytical data obtained by pXRF ('total') methods (Kjarsgaard et al., 2013).



Figure 7: Example of split drill core for used for pXRF, fusion and 4-acid laboratory analysis. Outer curved surface (left) and inner cut surface (right). The three black dots on the right core image indicate where pXRF analyses were obtained. A core depth of 17.1m is marked on the core, which corresponds to a wireline depth of 16.7m. Core sample length 7.0cm. Photographs by L.C. Olson. NRCan photograph DB numbers: 2022-307 (left image); 2022-308 (right image).

## **Data Delivery**

Data delivery is provided through a series of nested folders and files as detailed in the of\_8913\_read\_me file. For the laboratory methods data, lithium fusion total whole rock characterization method is represented by LF200 data and multi-acid ultra-trace is represented by MA250 data. The chemostratigraphic profiles display single element trends from the base to the top of the borehole. It is important to note that precision and accuracy are affected by concentration. Lower concentrations, especially those near the limit of detection (LOD) tend to result in lower precision, and thus higher % relative standard deviation (RSD).

Appendix A: All analytical data in Microsoft Excel format and column heading explanation file

Appendix B: pXRF versus laboratory geochemistry cross-plots

Appendix C: Chemostratigraphic logs

Appendix D: Core photographs

## **Data Processing**

To ensure the integrity of the geochemical data, the laboratory and pXRF data files were saved for reference (Appendix A: Raw Data spreadsheet) while copied files were used for data processing and calibration calculations. The pXRF data were examined for run time errors to ensure that each analysis ran for the full 180 seconds. Geochemical outliers and obvious errors were not observed. For downhole data plotting purposes (chemostratigraphy) results below the LOD, were given a value of half the recommended LOD. For example, pXRF LOD for Mg is 6000 ppm thus a value of 3000 ppm was substituted for the data point on the chemostratigraphic logs. The 30 core samples analyzed by both laboratory methods and pXRF spectrometry were compared on a series of x-y scatter plots to evaluate the accuracy of the pXRF data (Figure 8, see Appendix B). The laboratory data were plotted on the x-axis, and the mean pXRF data on the y-axis. Note that the mean pXRF data represents three separate analytical locations on the same core section that was homogenized and analyzed by laboratory methods. For example, the three pXRF analytical locations shown in Figure 7 result in three different analytical results due to the change in mineralogy and grain size between the analytical sites (Si (ppm) = 358,097; 372,804; 422,035). However, the mean of the pXRF results (Si mean = 384,804 ppm) is close to the fusion laboratory results for the homogenized sample (Si = 402,975 ppm). See Appendix A for additional examples. Equations and  $r^2$  values for pXRF (y-axis) and lithium borate fusion (x-axis) are shown in Table 1 with data plots shown in Figure 8. The full set of comparison plots is shown in Appendix B. To obtain the equations used to calibrate the pXRF dataset, the axes of the fusion data were reversed and the mean pXRF data inserted for the x-value, as shown in Figure 9.

Table 1: Equations and  $r^2$  values for pXRF (y-axis) and lithium borate fusion (x-axis). Element concentrations are in ppm, values have not been adjusted for significant figures.

Element	$y=mx+b$	$r^2$
Al	$1.3888x + 2908.7$	0.9646
Ba	$0.8533x - 51.39$	0.9444
Ca	$0.8468x + 2959.7$	0.9653
Ce	$0.455x - 78.595$	0.7608
Cu	$2.0056x - 4.848$	0.9804
Fe	$1.2002x + 481.52$	0.9736
K	$1.0778x - 150.6$	0.9560
La	$0.2878x - 50.496$	0.6062
Mg	$3.0042x - 6210.6$	0.9557
Mn	$1.0613x + 123.16$	0.9358
Mo	$2.5288x - 3.362$	0.9397
Nb	$1.0568x + 1.0247$	0.8046
Nd	$0.1232x - 56.646$	0.4614
Ni	$0.4917x + 1.5669$	0.5642
P	$1.6081x - 75.17$	0.8273
Pb	$0.8963x + 0.2225$	0.3946
Pr	$0.0562x - 14.232$	0.3673
Rb	$2.1365x + 3.3044$	0.9534
Si	$0.9927x + 9986$	0.9739
Sr	$0.9969x + 31.537$	0.9718
Th	$0.0636x + 1.2801$	0.2885
Ti	$0.9321x + 1089.2$	0.8273
U	$0.5989x + 0.5696$	0.3977
Y	$1.117x + 4.1857$	0.8399
Zn	$1.0126x - 5.5331$	0.9027
Zr	$1.132x + 69.257$	0.7398

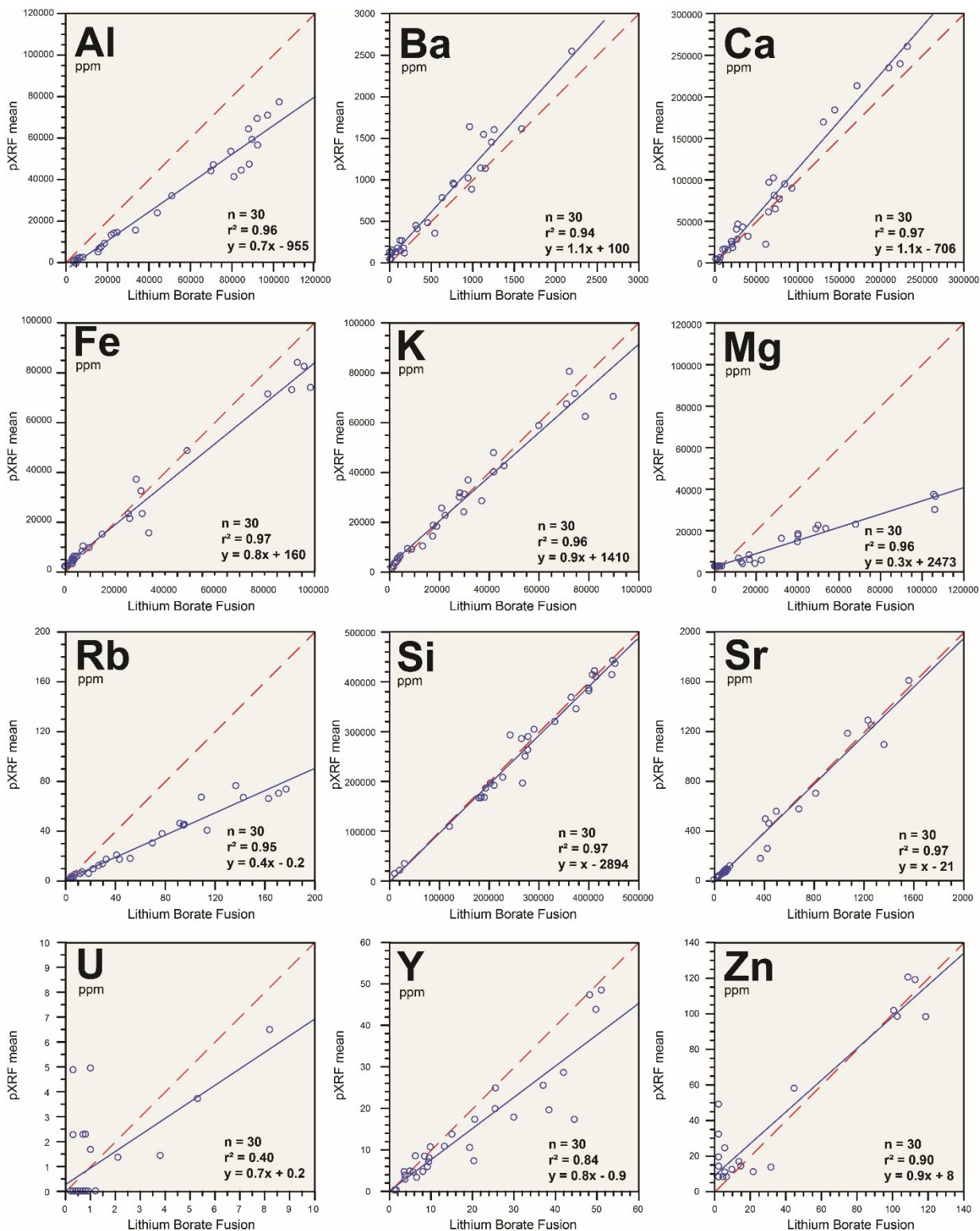


Figure 8: Illustrative elements of lithium borate fusion (x-axis) compared to the mean of three pXRF analyses (y-axis), where n is the number of comparative sample analyses. The red dashed line represents a one-to-one relationship, the blue line represents the regression equation.

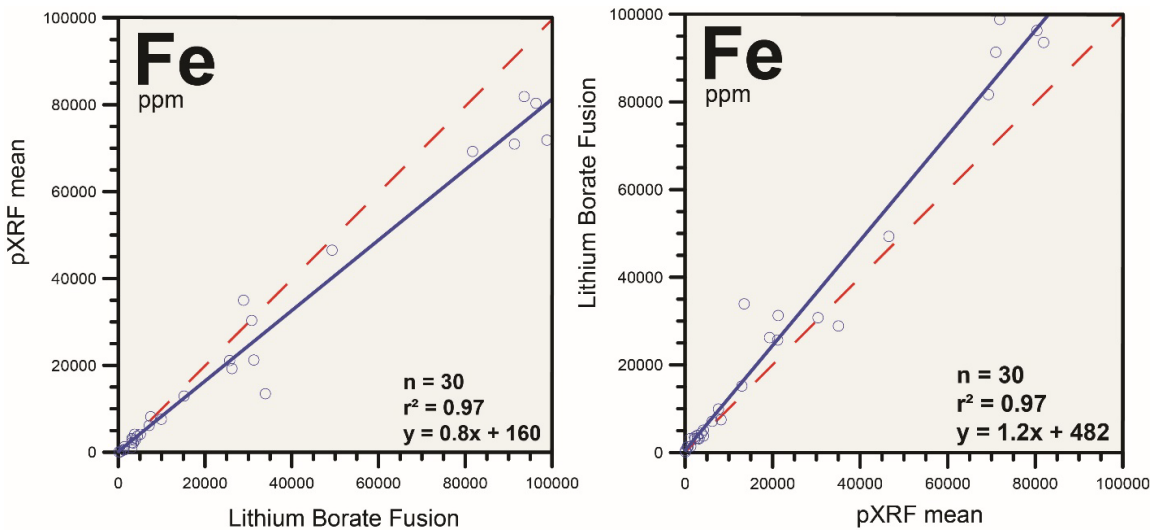


Figure 9: Example of exchanging the x and y axis to obtain a least-squares regression equation for calibration of the pXRF data to increase accuracy.

## 4.0 Geochemical Results

Geochemical variations detected are consistent with observed lithology as shown in Figure 4 and with downhole geophysical data presented in Figure 5 and Crow et al. (2021). Variations in most element concentrations such as Al, Ba, Ca, Fe, K, La, Mg, Mn, Ni, Pr, Rb, Si, Sr, Y and Zn were informative, while Mo, P, Pb, Th, Ti and Zr did not yield any significant chemostratigraphic information. Concentrations of Cu and U are near or below the LOD. A selection of elements that define the chemostratigraphy of borehole BC81-2 and the geophysical gamma responses are shown for comparison in Figures 10 and 11.

### Precambrian Bedrock (core depth 120.12 - 64.30m)

Precambrian rock from the base of the borehole to approximately 90m depth consists of a mafic mineral assemblage, with three significant syenite units and a thin layer of pegmatite. The mafic assemblage is shown by an increase in Fe, Mg, and Zn and a decrease in K and Si compared to the overlying rock. The concentration of K and Fe is relatively consistent and increases slightly from 120–90m. For elements such as, Ce, Fe, La, Mg, Mn, Nb, Nd, Y and Zn there is a sharp change in concentration at approximately 90m depth, and a more subtle change for Ca, Pr and Sr. From the base of the borehole to a depth of 90m Ni, Th show concentrations consistently above the detection limit compared to overlying rocks with lower values. Two of the three syenite units are defined by a sharp decrease in Ce, Fe, La, Mg, Mn, Nd, Ni, Pr, Y and Zn at roughly 116m and 100m depth. Concentrations of Al are highly variable with no apparent chemostratigraphic trend. From a depth of 100–98m the syenite unit shows a marked decrease in Ce, Fe, La, Nd, Pr, Y, and Zn with an increase in resistivity, and gamma and a corresponding significant decrease in density (Figs. 10, 11; Appendix C). Overall, the pXRF results are consistent with a transition from lowermost mafic ferromagnesium minerals (Fe and Mg) to overlying felsic Precambrian granites. This transition and change in rock chemistry is shown by an elevated responses in the resistivity, and density, and a lower gamma response than in the overlying granites (Figure 5). For these rocks, porosities are <0.5%, and bulk densities range from 2.70 to 3.05g/cm<sup>3</sup> (Crow et al., 2021).

Above 90m the lithology of the Precambrian rock is more felsic and shows decrease in Ce, Fe, La, Mg, Mn, Nd, Ni, P, Pr, Th, Y, and Zn. Compared to the underlying more mafic rocks, Si concentrations are slightly higher. The transition from mafic to more felsic rock is also shown in a decrease in density and an increase in gamma (Fig. 5 and Appendix C) however the transition occurs at a depth of ~94m, at the base of the upper syenite unit.

From the base of the borehole to approximately 70m, Mn, Ni and Zn decrease in concentration upwards until Mn and Ni are no longer detected, and Zn concentrations are near the LOD. Below the unconformity, there is a 17m-thick alteration zone that consists of sericite, chlorite, epidote, hematite and calcite, along with quartz and plagioclase associated with the underlying, unaltered, syenites and granites. The alteration zone is represented by an upward increasing trend and greater variability in K, Rb, Si and Zr concentrations compared to the underlying Precambrian rock and the overlying Keeseeville Fm. The increase in K concentration and gamma log counts is consistent with an increase in sericite and feldspar. These observations are consistent with potassic alteration. The presence of weathered clay minerals resulted in reduced readings for the induced polarization (IP) and resistivity responses (see Appendix C). The geophysical logs of Crow et al. (2021) show relatively low magnetic susceptibility response due to the alteration from magnetite to hematite. Porosity estimates range from 2.3% to 5.1%, and bulk densities from 2.50–2.62g/cm<sup>3</sup> (however note influence from weak samples in alternation zone during core testing).

The Precambrian regional unconformity with the overlying Keeseeville Fm. is sharp and observable as a change in concentration of most elements excluding Ca, Cu, Mn, Mo, Zn and Zr where the contact is either subtle or not detected.

### **Keeseeville Formation (core depth 64.30 - 20.45m)**

At the unconformity between the Precambrian and Keeseeville Fm., Ce, Mg, Nd, Pr, Sr, and Y show noticeable but subtle decreases in concentration, whereas Ca, Zn and Zr show little change in concentration. The basal quartz conglomerate unit and overlying white quartz arenite of the Keeseeville Fm show an abrupt decrease in concentration of Al, Ba, Fe, K, La and Rb, and a corresponding increase in Si compared to the underlying Precambrian rocks (Fig. 10 and 11). The geophysical data, (Fig. 5) indicate that the 5m interval above the Precambrian contact has low gamma response and is visibly more porous compared to the overlying sandstone. Porosities reported by Crow et al. (2021) ranged from 8.4% to 9.4% (2.38–2.40g/cm<sup>3</sup>).

Overall sandstones of the Keeseeville Fm show remarkably similar elemental concentrations indicating a homogeneous provenance. Exceptions occur between a depth of 46–44m where there is a consistent increase in Si concentration as well as an increase in Al, K, Nb, and Y. A second deviation from consistency in elemental concentrations occurs between a depth of 35–33m where there is an increase in Ca, K, La, Mn (above LOD), Nd, and a marked decrease in Si concentration. This deviation in elemental concentrations corresponds to a marked increase in the density log (Fig. 5, Appendix C).

From a depth of approximately 33m to the top of the Keeseeville Fm., Si concentration are similar to those in the quartz arenite from the base of the formation. For these upper quartz arenites Al, Ba, K, and Rb display a gradual curved shaped decrease in concentration similar to the pattern observable in the gamma and density responses (Fig. 5, Appendix C). Within the upper quartz arenite, porosity ranged from 1.5% (2.57g/cm<sup>3</sup>) to 12% (2.44g/cm<sup>3</sup>) and can change over short (decimeter-scale) vertical intervals (Crow et al., 2021). The geophysical data in the upper part of the Keeseeville Fm. display lower levels of total gamma

counts, resistivity, and density compared with the rest of the borehole. In addition, U was not detected in the Keeseville Fm.

### **Theresa and Beauharnois Formations (core depth 5.30 – 20.45m)**

The Theresa and overlying Beauharnois formations consist of sandy dolomite, dolomite, and dolomitic sandstone. At the base of the Theresa Fm., there is an increase in U (creating a sharp increase in gamma counts), along with an increase in Ca and Cu, and the start of a decreasing trend in Si. The increase in Cu and U is attributed to the presence of thucolite (Charbonneau et al., 1975; Bernius, 1996). The increase in Ca concentration correlates with the increasing occurrence of carbonates in the Beekmantown Group. Above the contact with the Keeseville Fm. there is a sharp increase in the concentration of Ca, Ce, La, Mg, Mn, Nd and Pr as well as a greater variability in concentrations. This variability is consistent with geophysical observations by Crow et al. (2021), where IP, resistivity, density, and magnetic susceptibility logs showed a general increase and more variability in the Theresa Fm. relative to the underlying Keeseville Fm. Porosities reported by Crow et al. (2021) over a 22 cm-long sample range from 1.95 – 3.12% with bulk densities ranging from 2.56–2.61g/cm<sup>3</sup>. From approximately 18–16m depth, a sandy horizon is represented by a decrease in Ca and Mg concentration and an increase in Si concentration. Above approximately 13m, Mg increases sharply reflecting a significant increase in dolomite content in the upper sediments of the borehole. The local thickness of the Theresa Fm. has been interpreted to be about 10m, suggesting that the upper few metres of core could represent Beauharnois Fm. sediments. The exact depth of the contact is not clear due to the transitional nature of the Theresa Fm. to the overlying Beauharnois Fm. Comparing Mg concentrations to the average Mg concentration over the Theresa and Beauharnois formations indicates a change from above average Mg to below average Mg concentrations occurs at approximately 11m depth. The uppermost 2–3 m of the borehole, compared to the underlying sediments, show low concentrations of Al, K and Si and high concentrations of Ca and Mg, which suggest a dolomite horizon within the sandy dolostone.

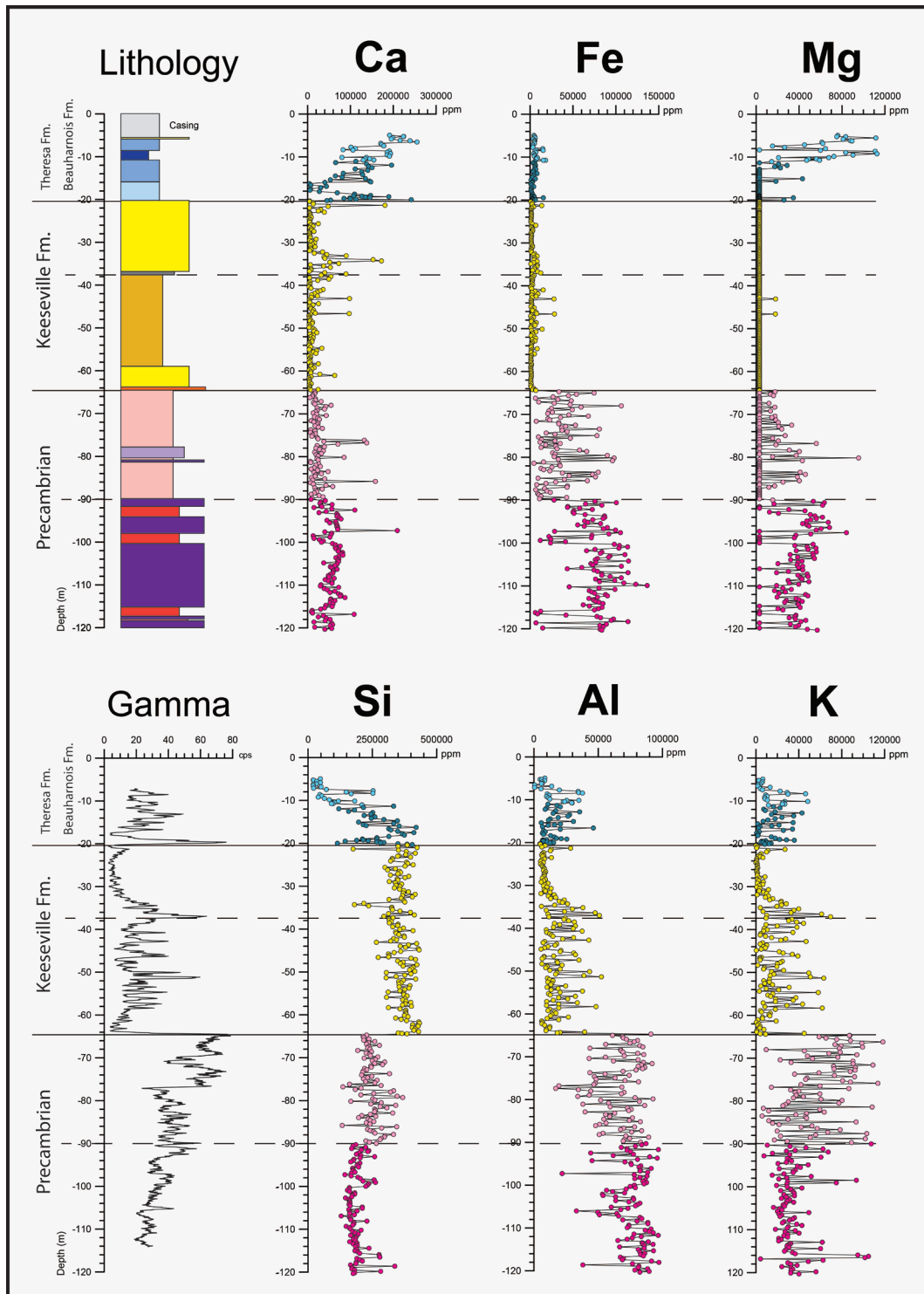


Figure 10: Lithology, select major element concentrations, and gamma count (cps x-axis) versus wireline depth. Pink markers represent Precambrian lithology (dark pink is more mafic, light pink more felsic). Yellow markers indicate quartz sandstone. Blue markers represent carbonate (dark blue has less carbonates, light blue more carbonates). See legend on Figure 4 for rock lithologies.

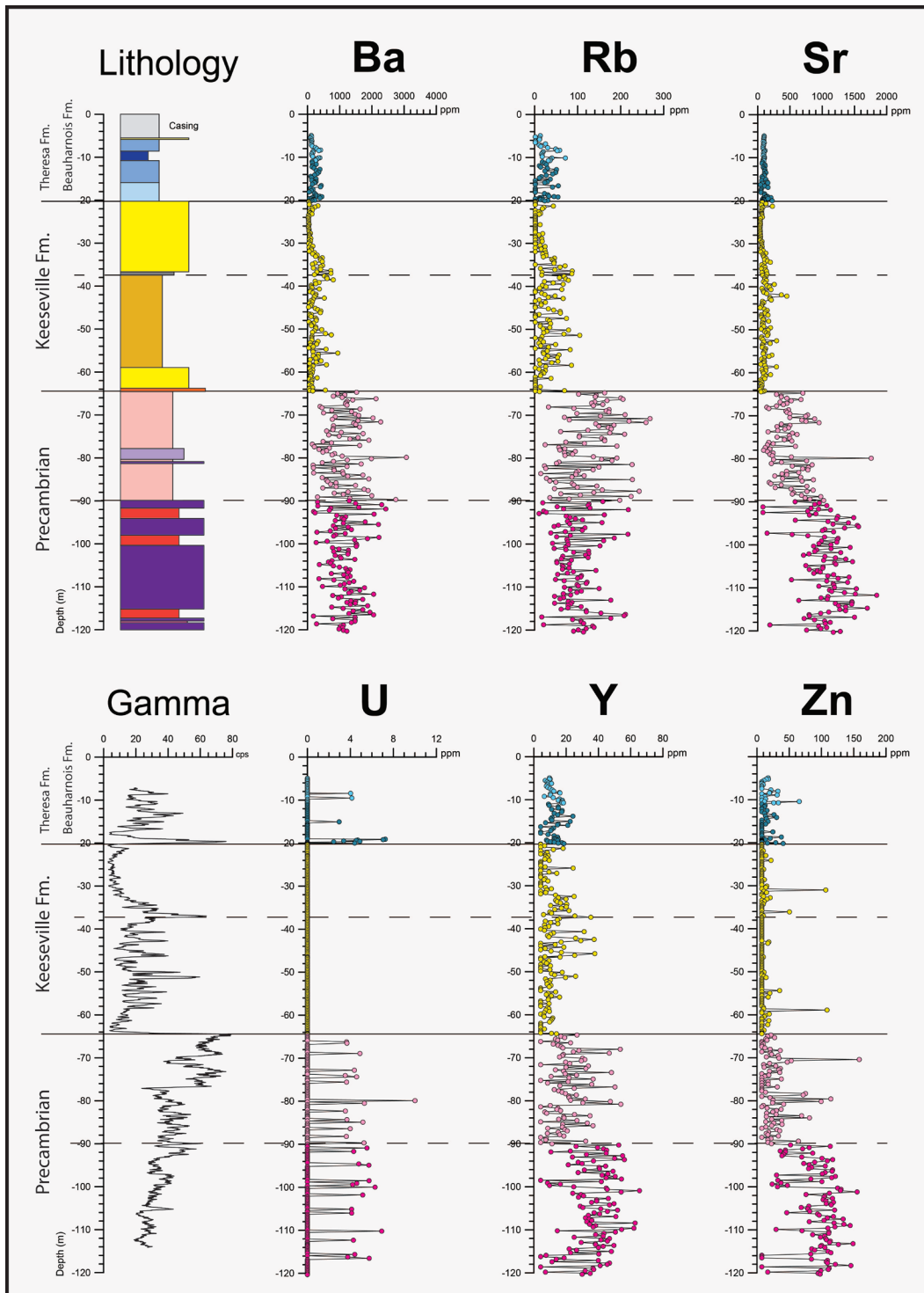


Figure 11: Select minor and trace elements that show significant changes in concentrations between rock types, formation boundaries, and gamma count (cps x-axis) versus wireline depth. Pink markers represent Precambrian lithology (dark pink is more mafic, light pink more felsic). Yellow markers indicate quartz sandstone. Blue markers represent carbonate (dark blue has less carbonates, light blue more carbonates). See legend on Figure 4 for rock lithologies.

## **5.0 Summary and conclusions**

This open file highlights chemostratigraphic observations obtained through analyses of rock core using pXRF spectrometry at a fraction of the cost of traditional laboratory analysis. This allowed for greater sampling density that led to observations on precise changes in lithology. Data acquired from this research augments and supports new data collected from the Bells Corners geophysical calibration site reported by Crow et al. (2021) and provide additional information on lithology and formation boundaries previously reported by Bernius (1996). The geochemical data from borehole BC81-2 provides an enhancement to the geophysical calibration data for the Precambrian basement and the overlying Keeseville, Theresa and Beauharnois Formations. The pXRF spectrometry methodology permitted an order of magnitude greater number of samples to be analyzed due to savings in cost related to core handling, processing, and laboratory analysis.

This research also highlights the validity of using pXRF spectrometry methods directly on rock core stored in core racks with minimal preparation. The procedures incorporated cleaning of the sample and ensuring a tight contact between the instrument window and the sample being analyzed. Results from this research further establish pXRF methods for the identification of subtle changes in rock lithologies, significant formation boundaries, and the presence of transition zones between formations. These methods have also shown that K alteration zones can be identified along with subtle changes in transitions between limestone and dolostone.

Finally, a subset of samples analyzed by pXRF spectrometry was subjected to traditional laboratory methods to verify the accuracy of the pXRF results and to provide a comparative basis to post calibrate pXRF data for enhanced accuracy.

## **6.0 Acknowledgements**

We would like to thank the Groundwater Geoscience Program of the Geological Survey of Canada (GSC) for supporting this research as part of the Archetypal Aquifer Project. We thank Alec Desbarats for providing helpful comments on the scientific content and structuring of a draft version of this report.

## **7.0 References**

- Bernius, G.R. 1996. Borehole geophysical logs from the GSC Borehole Geophysics Test Site at Bell's Corners, Nepean, Ontario. Geological Survey of Canada, Open File 3157. <https://doi.org/10.4095/207617>.
- Bernstein, L. 1992. A revised lithostratigraphy of the Lower-Middle Ordovician Group, St Lawrence Lowlands, Quebec and Ontario. Canadian Journal of Earth Sciences, 29: 2677-2694.
- Charbonneau, B.W., Jonasson, I.R., and Ford, K.L., 1975. Cu-U mineralization in the March Formation Paleozoic rocks of the Ottawa-St. Lawrence Lowlands. In Report of Activities, Part A, April to October 1974; Geological Survey of Canada, Paper no. 75-1A, pp. 229-233. <https://doi.org/10.4095/247867>.
- Chiarenzelli, J., Aspler, L.B., Donaldson, J.A., Rainbird, R., Mosher, D., Regan, S.P., Ibanez-Meija, M., and Franzi D.A. 2010. Detrital zircons of Cambro-Ordovician sandstone units in eastern Ontario and northern New York. Geological Society of America Abstracts with Programs, Vol. 42, No. 118.

- Corriveau, L., Heaman, L.M., Marcantonio, F., and van Breemen, O. 1990. 1.1 Ga K-rich alkaline plutonism in the SW Grenville Province. Contributions to Mineralogy and Petrology, 105: 473-485. <https://doi.org/10.1007/bf00286834>.
- Craigie, N., 2018. Principles of elemental chemostratigraphy: a practical user guide. Springer International Publishing. <https://doi.org/10.1007/978-3-319-71216-1>.
- Crow, H.L., Brewer, K.D., Cartwright, T.J., Gaines, S., Heagle, D., Pugin, A.J.-M., and Russell H.A.J. 2021. New core and downhole geophysical data sets from the Bells Corners Borehole Calibration Facility, Ottawa, Ontario. Geological Survey of Canada, Open File 8811. <https://doi.org/10.4095/328837>.
- Davidson, A. 1998. An overview of the Grenville Province geology, Canadian Shield, Chapter 3. In Geology of the Precambrian Superior and Grenville Provinces and Precambrian Fossils in North America. Ed. Lucas, S.B. and St-Onge, M.R.; Geological Survey of Canada, Geology of Canada, Series No. 7, pp. 205-270. <https://doi.org/10.4095/210103>.
- Di Prisco, G. and Springer, J.S. 1991. The Precambrian-Paleozoic unconformity and related mineralization in southeastern Ontario. Ontario Geological Survey, Open File Report 5751.
- Dix, G.R., Salad Hersi, O., and Nowlan, G.S. 2004. The Potsdam-Beekmantown Group boundary, Nepean Formation type section (Ottawa, Ontario): A cryptic sequence boundary, not a conformable transition. Canadian Journal of Earth Sciences, 41: 897-902.
- Easton, R.M. 1992. The Grenville Province and Proterozoic history of central and southern Ontario. In Geology of Ontario. Edited by P.C. Thurston, H.R. Williams, R.H. Sutcliffe, and G.M. Scott. Ontario Geological Survey, Special Volume 4, Part 2. pp. 715-904.
- Emmons, E. 1838. Report of the second geological district of the State of New York. New York Geological Survey, Annual Report, 2: 185-252.
- Glanzman, R.K., Closs, L.G., 2007. Field portable x-ray fluorescence geochemical analysis – its contribution to onsite real-time project evaluation. In: Proceedings of Exploration 07: Fifth Decennial International Conference on Mineral Exploration, pp. 291–301.
- Hoekstra, H.R. and Fuchs, L.H. 1960. The Origin of Thulcolite. Economic Geology, 55: 1716 – 1738.
- Hofmann, H.J. 1998. Synopsis of North American stratigraphic units with remains reported as pre-Cambrian, Figure 4-1. In Geology of the Precambrian Superior and Grenville Provinces and Precambrian Fossils in North America. Ed. Lucas, S.B. and St-Onge, M.R. Geological Survey of Canada, Geology of Canada, Series No. 7, pp. 205-270. <https://doi.org/10.4095/210103>.
- Killeen, P.G. and Conway, J.G. 1978. New facilities for calibrating gamma-ray spectrometric logging and surface exploration equipment, Canadian Institute of Mining and Metallurgical Bulletin, 793, pp. 84-87.

Killeen, P.G., Bernius, G.R., Schock, L., and Mwenifumbo, C. J. 1984. New developments in the GSC borehole geophysics test area and calibration facilities. In Current Research, Part B, Geological Survey of Canada, Paper 84-1B, pp. 373-374. <https://doi.org/10.4095/119597>.

Killeen, P.G. 1986. A system of deep test holes and calibration facilities from developing and testing new borehole geophysical techniques. In Borehole Geophysics for Mining and Geotechnical Applications. Edited by P.G. Killeen. Geological Survey of Canada, Paper 85-27, pp. 29-46. <https://doi.org/10.4095/123596>.

Kjarsgaard, B.A., Knight, R.D., Sharpe, D.R., Kerr, D.E., Cummings, D.I., Russell, H.A.J., Lemkow, D., Wright, D F, Bonham-Carter, G., 2013. Till geochemistry studies of the Thaidene Nene MERA study area. In: Ambrose, E.J., Lemkow, D. (Eds.), Mineral and Energy Resource Assessment of the Proposed Thaidene Nene National Park Reserve in the Area of the East Arm of Great Slave Lake, Northwest Territories. Geological Survey of Canada, pp. 313–337. <https://doi.org/10.4095/292459>. Open File 7196.

Knight, R.D., Klassen, R.A., and Hunt, P. 2002. Mineralogy of fine-grained sediment by energy-dispersive spectrometry (EDS) image analysis – a methodology, Environmental Geology, v. 42, n. 1, p. 32-40.

Knight, R.D., Kjarsgaard, B.A., and Russell H.A.J. 2021. An analytical protocol for determining the elemental chemistry of Quaternary sediments using a portable X-ray fluorescence spectrometer. Applied Geochemistry, 131: 1-15.

Landing E., Amati L., and Franzi D.A. 2009. Epeirogenic transgression near a triple junction; the oldest (latest Early-Middle Cambrian) marine onlap of cratonic New York and Quebec. Geological Magazine, 146: 552–566.

Lawley, C J M; Dubé, B; Mercier-Langevin, P; Kjarsgaard, B; Knight, R. D.; Vaillancourt, D., 2015. Defining and mapping hydrothermal footprints at the BIF-hosted Meliadine gold district, Nunavut, Canada. Journal of Geochemical Exploration, vol.155, p.35-55.

Lemiere, B. 2018. A review of pXRF (field portable X-ray fluorescence) applications for applied geochemistry. Journal of Geochemical Exploration, 188: 350–360. <https://doi.org/10.1016/j.jexplo.2018.02.006>.

Lowe, D.G. 2016. Sedimentology, stratigraphic evolution and provenance of the Cambrian-Early Ordovician Potsdam Group in the Ottawa Embayment and Quebec Basin. Ph.D. thesis, Department of Earth Sciences, University of Ottawa, Ontario.

Lowe, D.G., Arnott, R.W.C, Chiarenzelli, J.R., and Rainbird, R.H. 2018. Early Paleozoic rifting and reactivation of a passive-margin rift: Insights from detrital zircon provenance signatures of the Potsdam Group, Ottawa graben. GSA Bulletin, 130: 1377-1396.

Mwenifumbo, C.J., Elliott, B.E., Hyatt, W.G., and Bernius, G.R. 2005. Bells Corners calibration facilities for downhole and surface geophysical equipment. Geological Survey of Canada, Open File 4838. <https://doi.org/10.4095/216755>.

Pehme, P., Crow, H.L., Parker, B., and Russell, H.A.J. 2022. Evaluation of slim-hole NMR logging for hydrogeologic insights into dolostone and sandstone aquifers. *Journal of Hydrogeology*, <https://doi.org/10.1016/j.jhydrol.2022.127809>

Rouillon, M. and Taylor, M. 2016. Can field portable X-ray fluorescence (pXRF) produce high quality data for application in environmental contamination research? *Environmental Pollution*, 214: 225–264. <https://doi.org/10.1016/j.envpol.2016.03.055>.

Salad Hersi, O., Lavoie, D., Hilowle Mohamed, A., and Nowlan, G.S. 2002. Subaerial unconformity at the Potsdam–Beekmantown contact in the Quebec Reentrant: regional significance for the Laurentian continental margin history. *Bulletin and Canadian Petroleum Geology*, 50: 419-440.

Salad Hersi, O., Lavoie, D., and Nowlan, G.S. 2003. Reappraisal of the Beekmantown Group sedimentology Quebec: implications for understanding the depositional evolution of the Lower-Middle Ordovician Laurentian passive margin of eastern Canada. *Canadian Journal of Earth Sciences*, 40: 149-176.

Sanford, B.V. 2007. Stratigraphic and structural framework of the Potsdam Group in eastern Ontario, western Quebec and northern New York State. Ph.D. thesis, Department of Earth Sciences, University of Ottawa, Ontario.

Sanford, B.V. and Arnott, R.W.C. 2010. Stratigraphic and Structural Framework of the Potsdam Group in eastern Ontario, western Quebec and northern New York State. Geological Survey of Canada, Bulletin 597, Geological Survey of Canada, Ottawa, Ontario. <https://doi.org/10.4095/247669>.

Wynne-Edwards, H.R. 1972. The Grenville Province. *Geological Association of Canada Special Paper* 11: 163-182.